The M_W 5.9 Woods Point Earthquake: A Preliminary Investigation of the Ground Motion Observations

Ryan D Hoult[1], Adam Pascale[2], Abraham Jones[3], Trevor Allen[4]

1. *Institute of Mechanics, Materials and Civil Engineering, UCLouvain, Louvain-la-Neuve, Belgium.*
2. *Seismology Research Centre, Richmond, Victoria, Australia*
3. *School of Geography, Earth and Atmospheric Sciences, Faculty of Science, University of Melbourne, Parkville, Victoria, Australia*
4. *Geoscience Australia, Canberra, Australian Capital Territory, Australia*

Abstract

The 22 September 2021 (AEST) moment magnitude M_W 5.9 Woods Point earthquake was the largest in the state of Victoria's recorded history. The ground motions were felt throughout the state of Victoria and into neighbouring states New South Wales and South Australia. Minor damage was reported in the city of Melbourne and in some regional centres close to the epicentre. This event was captured on many high-quality recorders from multiple sources, including private, university, and public networks. These recordings provide a rare opportunity to assess the utility of some ground motion models thought to be applicable to the southeast region of Australia. This paper presents spectral acceleration and attenuation comparisons of the Woods Point earthquake relative to a selection of ground motion models. The results of this paper provide further evidence that the attenuation characteristics of southeastern Australia may be similar to that in central and eastern United States, particularly at shorter distances to the epicentre.

Keywords: ground-motion model, attenuation, seismic, models

1 Introduction

Ground motion models (GMMs) typically estimate the 5% damped spectral acceleration as a function of the period of vibration for an earthquake of given moment magnitude (M_W), depth, distance, and local site condition (Power *et al*., 2008; Bozorgnia *et al*., 2014; Goulet *et al*., 2021). In low-to-moderate and stable continental regions, such as Australia, the observed ground motion datasets are typically not sufficient to develop reliable GMMs based solely on the recorded data. Thus, it is common to adopt GMMs from other regions around the world that are well developed (e.g., California) and apply them for seismic hazard applications for regions in Australia. However, there have been some attempts at developing GMMs specifically for the Australian conditions (e.g., Allen, 2012; Lam *et al*., 2000; Somerville *et al*., 2009; Tang *et al*., 2020). Some deliberation amongst the engineering and seismology community in Australia over the past decade has focused on the selection and the associated weighting of the GMMs used in a probabilistic seismic hazard analysis (PSHA) (Burbidge, 2012; Hoult et al., 2013; Leonard et al., 2013, 2014; Lam et al., 2016; Griffin et al., 2018; Tang et al., 2019; Allen et al., 2020). Whilst several studies have investigated various GMMs for the Australian conditions (Brown et al., 2001; Burbidge, 2012; Hoult et al., 2014, 2019; Ghasemi and Allen, 2018), there has been a paucity of comprehensive studies that have explored the applicability of these GMMs by comparing the predictions to recordings of events. Recently, Hoult *et al*. (2021) evaluated several GMMs in comparison to the ground motion recordings of the M_W 5.1 Moe earthquake. It was found that, while some GMMs provided reasonably good estimates to the attenuation of the Moe earthquake ground motions, additional data was necessary to more thoroughly characterise the GMM logic trees for use in PSHAs (Hoult *et al*., 2021).

The 22 September 2021 M_W 5.9 Woods Point earthquake occurred at 9:15 a.m. local time (Australian Eastern Standard Time [AEST]) and was the largest in the state of Victoria's recorded history. The event was located some 12 km northeast of the small regional town of Woods Point and approximately 130 km northeast of Victoria's capital city of Melbourne. Minor damage to residential and commercial structures was observed close to the central business district of the city of Melbourne and some of neighbouring rural towns closer to the epicentre. The event was also widely felt throughout the state and into the neighbouring states of South Australia and New South Wales. The resulting Modified Mercalli Intensity (MMI) contour map is given in Figure 1, which was developed from ShakeMap (Wald *et al*., 1999; Wald *et al*., 2005), calibrated by almost 43,000 felt reports (e.g., Allen *et al*., 2019). The 2021 Woods Point earthquake was well recorded on private, university, and publicly funded seismic networks, with several high-quality ground-motion recordings within 200 km of the earthquake's epicentre. Unfortunately, the event caused ground vibrations that resulted in many of the weak-motion seismographs close to the epicentre to saturate, meaning that peak ground motions could not be measured reliably. Nevertheless, the many other high-quality recordings of this large earthquake make it one of the best recorded and most significant events in southeastern Australia (SEA). As discussed previously, one of the key challenges in addressing the uncertainty that is associated with the selection and weighting of GMMs is the paucity of recorded ground motion data in Australia (Allen, 2020). Thus, the recordings resulting from the Wood Points earthquake have provided a rare opportunity to evaluate GMMs that are thought to be applicable to the SEA region. These studies are important for potentially improving hazard estimates (and reducing their uncertainties) for the SEA region when using a PSHA, which is dependent on the GMMs used.

This research paper provides a preliminary observation of the ground motions recorded from the M_W 5.9 event in Victoria. Spectral acceleration and attenuation plots are provided for all of

the valid ground motions recorded, which are compared to a selection GMMs thought to be applicable for SEA.

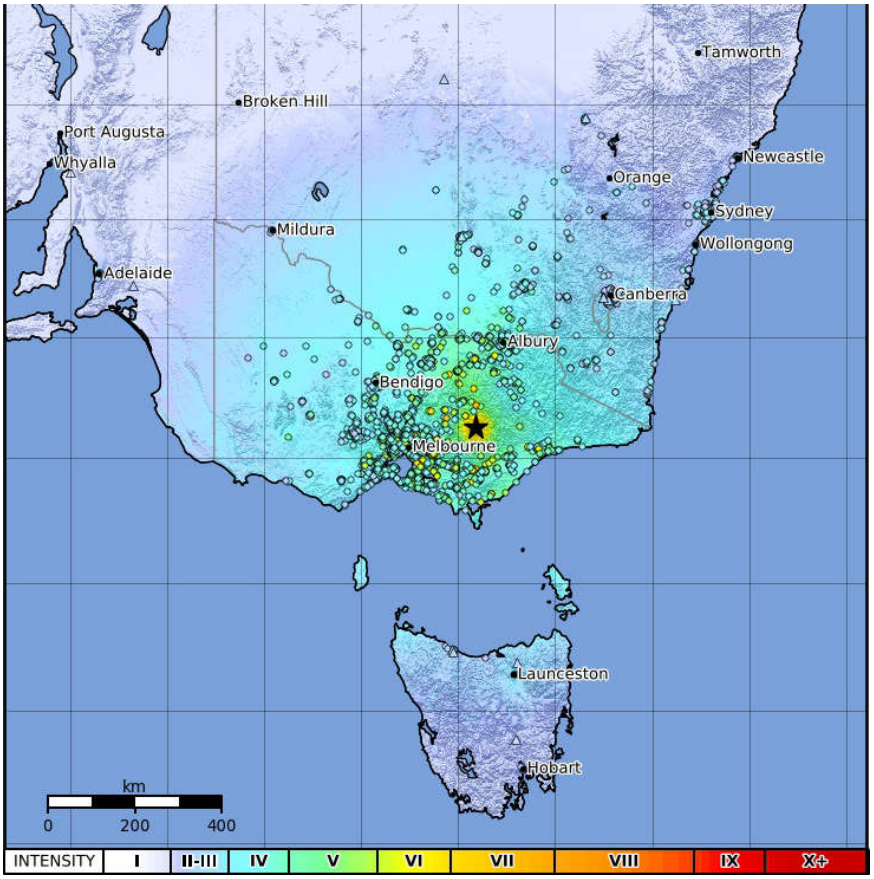

Figure 1 Modified Mercalli Intensity (MMI) ShakeMap generated by the M_W 5.9 22 September 2021 event (Geoscience Australia, 2021).

2 Recordings of the M_W 5.9 Main Event

In total, 61 recordings of the 22 September 2021 earthquake event have been obtained within a hypocentral distance of $R_{hyp} \leq 1000$ km. These ground motions were compiled from five different sources: Geoscience Australia (GA), Seismology Research Centre (SRC), the Australian National University's Seismometers in Schools (S1; Balfour *et al*., 2014), the University of Melbourne (UoM), and the Seismological Association of Australia (SAA). Table A1 provides the station names, networks, station locations, and peak ground acceleration (PGA) for the M_W 5.9 event. It should be noted that, for many of the recordings, the estimated high frequency limit was lower than 100 Hz, which is the frequency commonly used to approximate the PGA. Table A1 indicates that estimated high frequency limit for each of the recordings, which was taken as 40% of the sampling rate (or 80% of Nyquist). The location of the recording stations across the state of Victoria relative to the epicentre of the M_W 5.9 Woods Point earthquake is given in Figure 2.

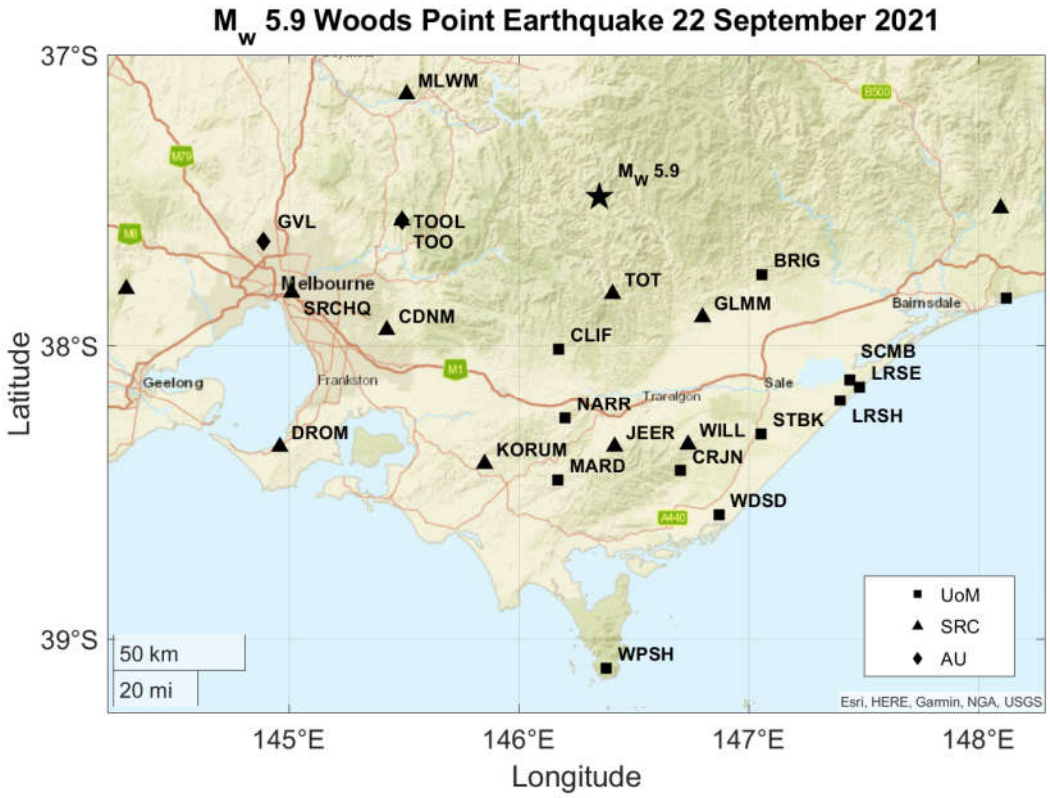

Figure 2 Location of several stations in the state of Victoria, Australia that recorded the M_W 5.9 Woods Points earthquake on 22 September 2021 (epicentre indicated with black star).

3 Spectral Comparisons

For the available recordings (Table A1), 5%-damped pseudo-response spectral acceleration was calculated over the full earthquake coda. All waveforms were filtered using a fourth-order lowpass Butterworth filter with a cut-off frequency determined by the Nyquist frequency of the record. The response spectra have been calculated as the geometric mean of the two horizontal components. Only the vertical component or one of the horizontals could be attained for some stations at the time of writing this paper; these stations are noted in Table A1. Furthermore, some of the sensors have a flat frequency response from 1 Hz (or 2 Hz) to 100 Hz, and acceleration readings for frequencies below 1 Hz (i.e., T > 1.0s) are not accurate if one does not account for the frequency-dependent response of the sensor (e.g., Scherbaum, 1996). As such, these sensors, which are indicated in Table A1, have a spectral acceleration limit corresponding to a period T of less than 1.0 s in the corresponding plots.

The spectral acceleration is plotted as a function of period of vibration in Figures 3 and 4 for the stations within a 250 km radius from the epicentre. Spectral acceleration estimates for seven GMMs considered suitable for seismic hazard assessments in eastern Australia are superimposed on these spectral plots: Atkinson and Boore (2006; AB06) for eastern North America; Somerville *et al*. (2009; Sea09) for non-cratonic regions of Australia (i.e., SEA); Allen (2012; A12) for SEA conditions; Boore *et al*. (2014; Bea14) for active tectonic regions; Chiou and Youngs (2014; CY14) for shallow crustal earthquakes in active tectonic environments; Tang *et al*. (2020; Tea20) for SEA based on MMI data (Tang *et al*., 2019); and the Next Generation Attenuation (NGA)-East GMM for central and eastern North America (Goulet *et al*., 2021). Some of these GMMs were selected primarily due to the results of the expert elicitation of model parameters that were used for the development of the 2018 National Seismic Hazard Assessment in Australia (Ghasemi and Allen, 2018; Griffin *et al*., 2018). Importantly, it is assumed that all of the recording stations used here are sited on rock-type conditions (i.e.,

shear wave velocity [V_{S30}] of approximately 760 m/s). While this is unlikely to be the case (i.e., see Hoult *et al*., 2021), further research is required to determine the V_{S30} for each of the sites and correspondingly the amplification factors to apply to the GMMs used here.

The NGA-East model is observed to be the only GMM that can reasonably predict the short-period ground motions for some of the records in Figure 3 and 4. This suggests that there may be similarities between the source and attenuation properties between central and eastern United States (CEUS) and SEA, which contrasts the findings in Hoult *et al*. (2021) for comparisons with the M_W 5.1 Moe earthquake. Some previous research suggests that the source and attenuation properties between CEUS and SEA are comparable at short-distance ranges (i.e., R_{hyp} < 70 km) (Allen and Atkinson, 2007).

4 Attenuation Comparisons

Figure 5 presents the recorded spectral accelerations as a function of the Joyner-Boore (R_{JB}) distance of the 22 September 2021 M_W 5.9 event at six different periods: 0.01 (approximately, *PGA*), 0.1, 0.2, 0.5, 1.0, and 2.0 s. Superimposed in these figures are the spectral acceleration estimates as a function of the R_{JB} distance from the seven GMMs (listed in Section 3) assuming a V_{S30} of 760 m/s. As previously discussed in Section 3, in the absence of accounting for the frequency-dependent response of the sensor (e.g., Scherbaum, 1996), some of the recordings listed in Table A1 are currently limited to readings above 1 Hz (i.e., T < 1.0s); as such, the data from these recordings has not been included in Figure 5f.

Various GMMs appear to provide reasonable estimates of the attenuation of the ground motions for the large earthquake event. The following discussions appear to be consistent with the findings in Hoult *et al*. (2021) for the M_W 5.1 earthquake event. The GMMs developed for central and/or eastern North America (i.e., NGA-East and AB06) appear to intersect the majority of the data and particularly for high frequencies. Three GMMs specifically developed for SEA, A12 and Tea19, also appear to reasonably predict the attenuation, particularly for lower frequencies. As discussed in Hoult *et al*. (2021), the GMMs that incorporate an attenuation "transition zone" due to the strong postcritical reflections from the Moho discontinuity (Atkinson, 2004) have previously been shown to perform well for Fourier spectral amplitudes at short distances when compared to recorded data from SEA. It appears that this is consistent with the M_W 5.9 Woods Point earthquake event (i.e., AB06, A12, and NGA-East in Figure 5d for R_{JB} > 100 km). What is evident for the data plotted in Figure 5e is the above-average high-frequency content from this earthquake in comparison to the accelerations recorded in the low-frequency range (i.e., T=1.0s).

5 Conclusions

The 22 September 2021 M_W 5.9 Woods Point earthquake event was felt throughout the states of Victoria, South Australia, and New South Wales, causing minor damage in Melbourne and in neighbouring towns close to the epicentre, such as Mansfield, Benalla and Wangaratta. There were many recordings of this event from multiple sources, which provides a rare opportunity to analyse ground motions from large earthquakes in southeastern Australia. A range of GMMs tested against the data appeared to provide reasonable estimates. Whilst the assumption of a uniform site condition is an important limitation (i.e., V_{S30} = 760 m/s), the NGA-East GMM, which is calibrated to a V_{S30} of 3,000 m/s, appears to do a reasonable job at predicting the large accelerations observed in the short-period range (T < 0.1 s) range for some of the recordings. However, it is important to note that the use of the NGA-East GMM for lower V_{S30} will yield larger short-period accelerations, by about 10-20%, when converted to a

reference site condition 760 m/s. The recommended linear correction in the mid-period range ($0.1 \leq T < 1.0$ s) will be larger than 50% for some periods (Stewart *et al.*, 2020).

The preliminary spectral acceleration and attenuation comparisons to the GMMs in this paper provide further evidence that source and attenuation properties between central and eastern United States and southeastern Australia may be similar, particularly within short distances from the epicentre. While studies such as this are important for future seismic hazard studies, multiple-event strong- and weak-motion data are required to be evaluated before any scientifically defensible recommendations can be made to define ground-motion characterisation models for future PSHAs. Furthermore, as of writing this paper, more ground motion data are being sought from a range of different sources, which may provide additional observations and evidence that can help validate GMMs for improving future hazard studies.

6 Acknowledgments

The authors are grateful to Hadi Ghasemi for his thoughtful comments on this manuscript. Trevor Allen publishes with the authorisation of the CEO of Geoscience Australia.

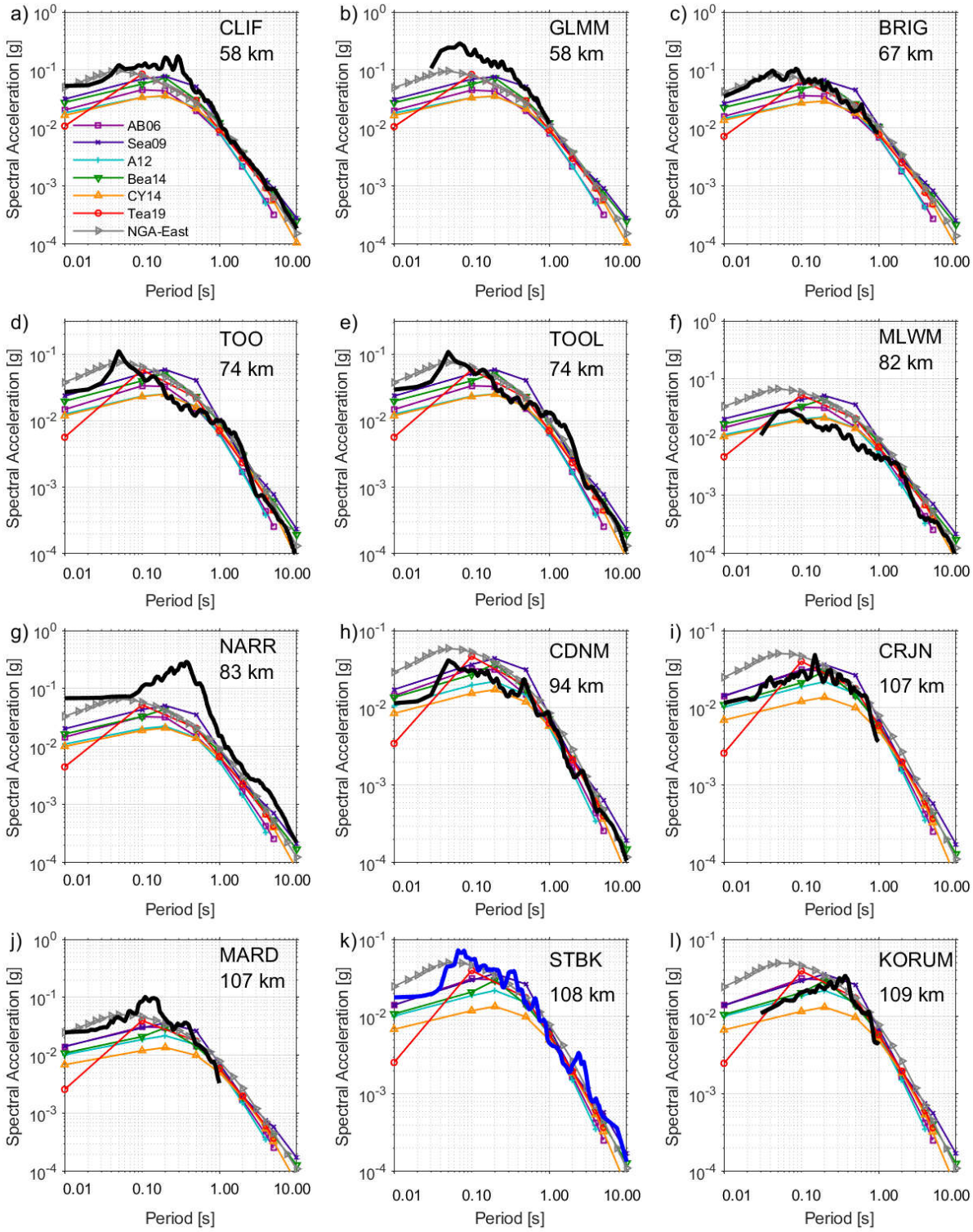

Figure 3 Five percent damped pseudoresponse spectral acceleration for the 22 September 2021 M_w 5.9 earthquake plotted relative to published GMMs considered for use in SEA. Black lines represent the geometric mean of the horizontal recordings, whereas blue lines represent the vertical response only.

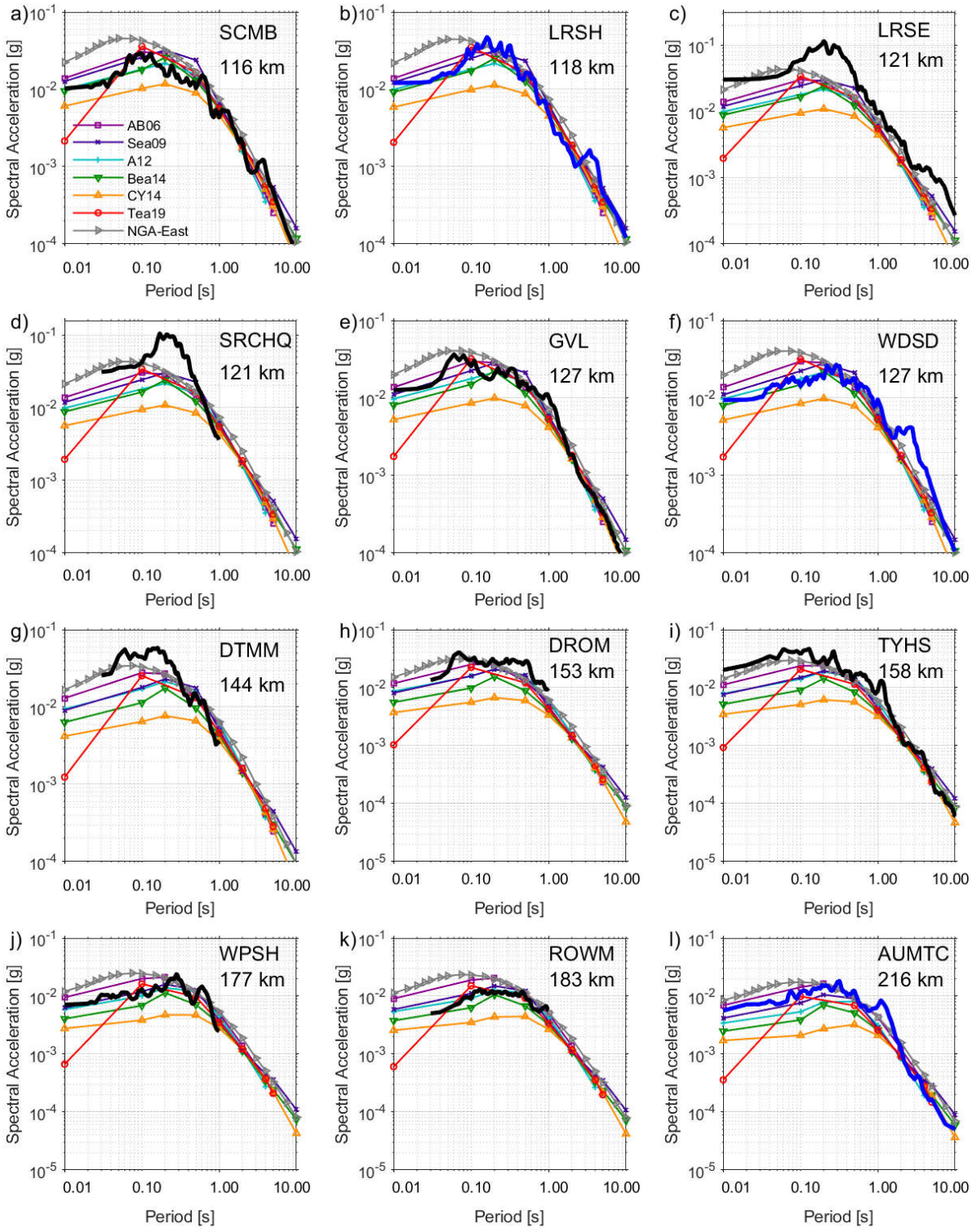

Figure 4 Five percent damped pseudoresponse spectral acceleration for the 22 September 2021 M_w 5.9 earthquake plotted relative to published GMMs considered for use in SEA. Black lines represent the geometric mean of the horizontal recordings, whereas blue lines represent the vertical response only.

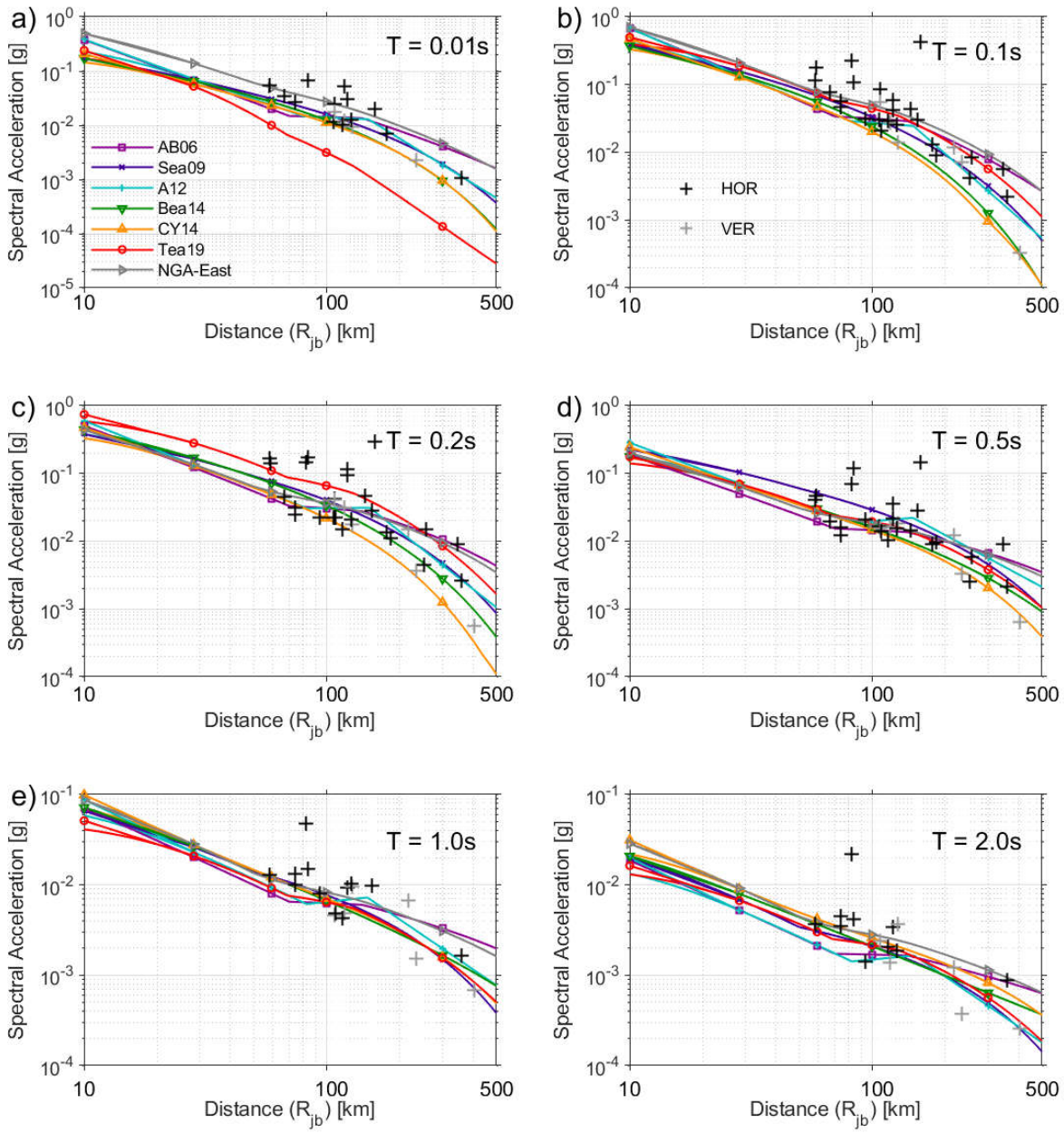

Figure 5 Attenuation of ground motions for the 22 September 2021 M_w 5.9 event is presented with the spectral acceleration a function of the Joyner-Boore distance (R_{JB}) for six periods: (a) T=0.01, (b) T=0.1, (c) T=0.2, (d) T=0.5, (e) T=1.0, and (f) T=2.0 s. Black plus sign ("+") markers correspond to horizontal responses, whereas the grey markers correspond to vertical component only.

7 References

Allen, T. (2012). Stochastic ground motion prediction equations for southeastern Australian earthquakes using updated source and attenuation parameters. *Geoscience Australia Record 2012/69*, Canberra, pp 55.

Allen, T., A. Carapetis, J. Bathgate, H. Ghasemi, T. Pejić, & A. Moseley (2019). Real-time community internet intensity maps and ShakeMaps for Australian earthquakes, *Australian Earthquake Engineering Society 2019 Conference*, Newcastle, New South Wales.

Allen, T. I., Griffin, J. D., Leonard, M., Clark, D. J., & Ghasemi, H. (2020). The 2018 national seismic hazard assessment of Australia: Quantifying hazard changes and model uncertainties. *Earthquake Spectra*. *36*(S1), 5-43. doi:10.1177/8755293019900777

Allen, T. I. (2020). Seismic hazard estimation in stable continental regions. *Bulletin of the New Zealand Society for Earthquake Engineering*, *53*(1), 22-36.

Atkinson, G. M. (2004). Empirical attenuation of ground-motion spectral amplitudes in southeastern Canada and the northeastern United States. *Bulletin of the Seismological Society of America*, *94*(3), 1079-1095.

Atkinson, G. M., & Boore, D. M. (2006). Earthquake Ground-Motion Prediction Equations for Eastern North America. *Bulletin of the Seismological Society of America, 96*(6), 2181-2205. doi:10.1785/0120050245

Balfour, N. J., Salmon, M., & Sambridge, M. (2014). The Australian seismometers in schools network: Education, outreach, research, and monitoring. *Seismological Research Letters*, *85*(5), 1063-1068.

Boore, D. M., Stewart, J. P., Seyhan, E., & Atkinson, G. M. (2014). NGA-West2 equations for predicting PGA, PGV, and 5% damped PSA for shallow crustal earthquakes. *Earthquake Spectra, 30*(3), 1057-1085. doi:10.1193/070113EQS184M

Bozorgnia, Y., Abrahamson, N. A., Atik, L. A., Ancheta, T. D., Atkinson, G. M., Baker, J. W., . . . Youngs, R. (2014). NGA-West2 Research Project. *Earthquake Spectra, 30*(3), 973-987. doi:10.1193/072113EQS209M

Brown, A., Allen, T., & Gibson, G. (2001). *Seismicity and earthquake hazard in gippsland.* Paper presented at the Australian Earthquake Engineering Society Conference, Canberra, Paper 22.

Burbidge, D. R. (2012). The 2012 Australian Earthquake Hazard Map. In *Record 2012/71*: Geoscience Australia: Canberra.

Chiou, B. and R. Youngs, *Update of the Chiou and Youngs NGA Model for the Average Horizontal Component of Peak Ground Motion and Response Spectra.* Earthquake Spectra, 2014.

Geoscience Australia (Cartographer). (2021). Earthquake Details, N of Rawson, VIC, 22/09/2021 09:15:53. Retrieved from https://earthquakes.ga.gov.au/event/ga2021sqogij

Ghasemi, H., & Allen, T. I. (2018). Selection and ranking of ground-motion models for the 2018 National Seismic Hazard Assessment of Australia: summary of ground-motion data, methodology and outcomes. *Geoscience Australia Record 2018/29*, 29. doi:10.11636/Record.2018.029

Goulet, C. A., Y. Bozorgnia, N. Kuehn, L. Al Atik, R. R. Youngs, R. W. Graves, & G. M. Atkinson (2021). NGA-East Ground-Motion Characterization model part I: summary of products and model development, *Earthq. Spectra* **37,** 1231–1282, doi: 10.1177/87552930211018723.

Griffin, J., Gerstenberger, M., Allen, T., Clark, D., Cuthbertson, R., Dimas, V.-A., . . . Venkatesan, S. (2018). *Expert elicitation of model parameters for the 2018 National Seismic Hazard Assessment: Summary of workshop, methodology and outcomes.*

Record 2018/28. Geoscience Australia, Canberra. Retrieved from doi:10.11636/Record.2018.028

Hoult, R. D., Lumantarna, E., & Goldsworthy, H. M. (2013). *Ground Motion Modelling and Response Spectra for Australian Earthquakes*. Paper presented at the Australian Earthquake Engineering Society 2013 Conference, Hobart, Tasmania.

Hoult, R. D., Amirsardari, A., Sandiford, D., Lumantarna, E., Goldsworthy, H. M., Gibson, G., & Asten, M. (2014). *The 2012 Moe Earthquake and Earthquake Attenuation in South Eastern Australia*. Paper presented at the Australian Earthquake Engineering Society 2014 Conference, Lorne, Victoria.

Hoult, R., Goldsworthy, H., & Lumantarna, E. (2019). Fragility Functions for RC Shear Wall Buildings in Australia. *Earthquake Spectra, 35*(1), 333-360. doi:10.1193/120717EQS251M

Hoult, R., Allen, T., Borleis, E., Peck, W., & Amirsardari, A. (2021). Source and Attenuation Properties of the 2012 Moe, Southeastern Australia, Earthquake Sequence. *Seismological Society of America*, *92*(2A), 1112-1128.

Lam, N., Wilson, J., Chandler, A., & Hutchinson, G. (2000). Response spectral relationships for rock sites derived from the component attenuation model. *Earthquake Engineering & Structural Dynamics, 29*(10), 1457-1489.

Lam, N. T. K., Tsang, H. H., Lumantarna, E., & Wilson, C. J. N. (2016). Minimum loading requirements for areas of low seismicity. *Earthquakes and structures, 11*(4), 539-561. doi:10.12989/eas.2016.11.4.539

Leonard, M., Burbidge, D., & Edwards, M. (2013). Atlas of seismic hazard maps of Australia: seismic hazard maps, hazard crurves and hazard spectra. In *Record 2013/41*: Geoscience Australia: Canberra.

Leonard, M., Hoult, R. D., Somerville, P., Sandiford, D., Gibson, G., Goldsworthy, H. M., . . . Spiliopoulos, S. (2014). *Deaggregating the differences between seismic hazard assessments at a single site.* Paper presented at the Australian Earthquake Engineering Society 2014 Conference, Lorne, VIC.

Power, M., Chiou, B., Abrahamson, N., Bozorgnia, Y., Shantz, T., & Roblee, C. (2008). An Overview of the NGA Project. *Earthquake Spectra, 24*(1), 3-21.

Scherbaum, F. (1996). *Of poles and zeros: fundamentals of digital seismology*, Dordrecht, Kluwer Academic Press, pp 256.

Somerville, P., Graves, R., Collins, N., Song, S. G., Ni, S., & Cummins, P. (2009). *Source and Ground Motion Models for Australian Earthquakes*. Paper presented at the Australian Earthquake Engineering Society 2009 Conference, Newcastle, New South Wales.

Stewart, J. P., G. A. Parker, G. M. Atkinson, D. M. Boore, Y. M. A. Hashash, & W. J. Silva (2020). Ergodic site amplification model for central and eastern North America, *Earthquake Spectra 36*(1), 42-68, doi: 10.1177/8755293019878185.

Tang, Y., Lam, N., Tsang, H.-H., & Lumantarna, E. (2019). Use of Macroseismic Intensity Data to Validate a Regionally Adjustable Ground Motion Prediction Model. *Geosciences, 9*(10), 422. doi:10.3390/geosciences9100422

Tang, Y., Lam, N., Tsang, H.-H., & Lumantarna, E. (2020). An Adaptive Ground Motion Prediction Equation for Use in Low-to-Moderate Seismicity Regions. *Journal of Earthquake Engineering*, 1-32. doi:10.1080/13632469.2020.1784810

Worden, C. B., E. M. Thompson, J. W. Baker, B. A. Bradley, N. Luco, & D. J. Wald (2018). Spatial and spectral interpolation of ground-motion intensity measure observations, *Bull. Seismol. Soc. Am.* 108**,** 866-875, doi: 10.1785/0120170201.

Wald, D. J., V. Quitoriano, T. H. Heaton, H. Kanamori, C. W. Scrivner, and C. B. Worden (1999). TriNet "ShakeMaps": Rapid generation of peak ground-motion and intensity maps for earthquakes in southern California, *Earthq. Spectra* **15,** 537-556, doi: 10.1193/1.1586057.

Wald, D. J., Worden, B. C., Quitoriano, V., & Pankow, K. L. (2005). *ShakeMap manual: technical manual, user's guide, and software guide* (No. 12-A1).

8 Appendix

Table A1 Seismometers and locations from epicentre of the 22 September 2021 M_w 5.9 event

Station Name	Network	Longitude (°)	Latitude (°)	R_{JB} (km)	*PGA* (g)	High Frequency Limit (Hz)
CLIF	UoM	146.1736	-38.0115	58	0.053	100
GLMM[3]	SRC	146.7989	-37.9026	58	-	40
BRIG[2,3]	UoM	147.0576	-37.7565	67	0.035	100
TOO	AU	145.4906	-37.5714	74	0.027	80
TOOL	SRC	145.4906	-37.5714	74	0.029	40
MLWM	SRC	145.5115	-37.1362	82	-	40
NARR	UoM	146.2024	-38.2496	83	0.068	100
CDNM	SRC	145.4252	-37.9465	94	0.011	40
CRJN[2,3]	UoM	146.7034	-38.4291	107	0.012	100
MARD[2,3]	UoM	146.1694	-38.4619	107	0.025	100
STBK[1]	UoM	147.0552	-38.3045	108	0.018	100
KORUM[3]	SRC	145.8509	-38.4065	109	-	40
SCMB[2]	UoM	147.4389	-38.1158	116	0.010	100
LRSH[1]	UoM	147.3977	-38.1891	118	0.012	100
LRSE[1]	UoM	147.482	-38.142	121	0.030	100
SRCHQ[3]	SRC	145.0114	-37.8189	121	-	40
GVL	AU	144.889	-37.64214	127	0.013	80
WDSD[1]	UoM	146.8701	-38.5798	127	0.009	100
DTMM[3]	SRC	147.4654	-36.5281	144	-	40
DROM[3]	SRC	144.9598	-38.3481	153	-	40
TYHS[2]	UoM	148.1193	-37.8363	158	0.020	100
WPSH[2,3]	UoM	146.3816	-39.0977	177	0.007	100
ROWM[3]	SRC	144.2918	-37.8061	183	-	40
AUMTC[1]	S1	143.8771	-37.6089	216	-	40
DEAL[1]	UoM	147.3137	-39.4725	234	0.002	100
HOPM[3]	SRC	144.2059	-35.9947	251	-	40
FRTM[3]	SRC	143.7177	-38.5319	256	-	40
RNDA[2]	UoM	149.0815	-35.2582	346	-	40
CNB	AU	149.3633	-35.315	360	0.0011	80
ARPS[1]	AU	141.8383	-36.7699	406	-	16
MGBR[1]	AU	140.571	-37.7283	508	-	16
WKA[2]	SAA	140.3225	-36.4158	547	-	40
ROBE[2]	SAA	139.8742	-37.1472	572	-	40
CMSA[1]	AU	145.6903	-31.539	662	-	16
SUND[2]	SAA	139.637	-34.6626	678	-	40
AUMBR[1]	S1	139.2859	-35.134	683	-	40
PLMR	SAA	139.1507	-34.8728	706	-	40
SDAN	AU	139.3374	-34.5093	710	-	16
STR2[2]	SAA	138.848	-35.2871	713	-	40

Station Name	Network	Longitude (°)	Latitude (°)	R_{JB} (km)	*PGA* (g)	High Frequency Limit (Hz)
TPSO	SAA	138.6373	-35.4895	722	-	40
HMV1	SAA	138.6372	-35.4894	722	-	40
UTT[2]	SAA	138.7367	-34.8215	743	-	40
DNL2	SAA	138.6431	-34.9014	747	-	40
DNL3	SAA	138.6431	-34.9014	747	-	40
DNL	SAA	138.6431	-34.9012	747	-	40
BRTS	SAA	138.5313	-35.0263	750	-	40
STKA[1]	AU	141.5952	-31.8769	758	-	16
HML1[2]	SAA	138.5889	-34.4034	776	-	40
PENW[2]	SAA	138.6208	-33.9293	800	-	40
HTT[1]	AU	138.9217	-33.4305	808	-	16
MRAT[1]	SAA	137.6256	-34.5272	849	-	40
KELC[1]	SAA	136.9111	-35.9825	855	-	16
WAL1[2]	SAA	137.6123	-34.1087	871	0.0001	100
WALR	SAA	137.6221	-33.9598	878	-	40
NAPP[1]	AU	138.145	-33.184	883	-	40
YAPP[1]	AU	138.3119	-31.8663	963	-	16
CLV2[2]	SAA	136.5169	-33.6823	982	-	40

[1]Vertical component only
[2]Horizontal component only (i.e., one channel, not mean of the two)
[3]Flat frequency response with accurate acceleration readings from 1Hz to 100Hz only